J Stomatol Oral Maxillofac Surg 127 (2026) 102598

Available online at ScienceDirect www.sciencedirect.com

Elsevier Masson France EM|consulte www.em-consulte.com

Original Article

# Effects of mandibular protrusion on the structural features of the masticatory muscles and upper airway space – a pilot study

Daria Madanchi [a], Catherine M. Paverd [b], Constantin von Deuster [c,d], Stefan Sommer [c,d], Marga B. Rominger [b], Dominik A. Ettlin [e,f], Luigi M. Gallo [a], Vera Colombo [a,*]

[a] Clinic of Masticatory Disorders and Dental Biomaterials, Center for Dental Medicine, University of Zurich, Zurich, Switzerland
[b] Zurich Ultrasound Research and Translation (ZURT), Institute of Diagnostic and Interventional Radiology, University Hospital Zurich, Zurich, Switzerland
[c] Swiss Center for Musculoskeletal Imaging (SCMI), Balgrist Campus AG, Zurich, Switzerland
[d] Advanced Clinical Imaging Technology (ACIT), Siemens Healthineers International AG, Zurich and Lausanne, Switzerland
[e] Department of Reconstructive Dentistry and Gerodontology, School of Dental Medicine, University of Berne, Berne, Switzerland
[f] Medical Sleep Experts, Schaffhauserstrasse 124, 8057 Zurich, Switzerland

ARTICLE INFO

*Keywords:*
OSA
MAD
Upper airway space
Streamline tractography
Masticatory muscle
Fiber orientation
MRI

ABSTRACT

*Objectives:* Obstructive Sleep Apnea (OSA) is the most common sleep breathing disorder. Treatment of mild to moderate OSA includes mandibular advancement devices (MAD). The varying degrees of mandibular protrusion induced by MADs affect the 3-dimensional arrangement of masticatory muscles. This pilot study aimed to observe the effects of different mandibular protrusions on masticatory muscle features and upper airways in one healthy participant.

*Study Design:* Anatomical and diffusion tensor imaging (DTI) magnetic resonance imaging (MRI) scans of the cephalic region of one 24-years-old healthy male subject were obtained with the mandible held stable by a personalized MAD in three positions: habitual bite position ($P_R = 0$ mm), middle protrusion ($P_{MID} = 3.5$ mm), maximum protrusion ($P_{MAX} = 7$ mm). Streamline tractography (ST) based on Spherical Deconvolution (SD) was performed. Anatomical masks for the masseter (superficial/deep), medial and lateral pterygoid, and temporalis muscles were manually drawn. The angles formed by each detected muscle fiber projected on coronal, sagittal, and axial planes were computed, and their distribution was calculated. Furthermore, airway volume and minimum cross-sectional area ($CSA_{MIN}$) for each position were determined.

*Results:* ST method captured the fiber orientation of all masticatory muscles. Variations in muscle fiber angles and airway space were observed across mandibular positions. Both airway volume and $CSA_{MIN}$ increased with increasing protrusion.

*Conclusions:* Mandibular protrusion affected the orientation and distribution of the masticatory muscle fibers and the upper airway space in the observed subject. These preliminary findings support further investigations into OSA patients.

## 1. Introduction

Obstructive sleep apnea (OSA) is a complex multifactorial disorder that causes a transient and repetitive partial or complete closure of the upper airways during sleep, resulting in sleep fragmentation and oxygen desaturation [1]. Apnea is defined as a reduction in airflow ≥ 90 % of baseline for more than 10 s [2]. Untreated OSA is associated with multiple adverse health outcomes, including systemic hypertension, coronary artery disease, stroke, atrial fibrillation, congestive heart failure, daytime sleepiness, reduced quality of life, and increased mortality [3–5].

The first-choice treatment for moderate to severe OSA is continuous positive airway pressure (CPAP) which helps maintain airway patency by supplying a forced airflow into the patients' mouth and nose [6,7]. The effectiveness of CPAP has been documented in several clinical trials, showing good results in the reduction of apnea episodes and improvement of quality of life [8,9]. Despite its efficacy, difficulties in tolerating this treatment may limit patients' compliance, which has been reported to be between 30 and 60 %, and therefore limit the benefits of the treatment [10,11].

An increase in the distance of the tongue base to the posterior pharyngeal wall has been observed with mandibular protrusion, and therapies based on this principle have been introduced in recent years as an alternative to CPAP. A mandibular advancement device (MAD) is an oral appliance consisting of an upper and lower dental splint. It is

*Corresponding author at: Plattenstrasse 11, CH, 8032 Zurich.
*E-mail address:* vera.colombo@zzm.uzh.ch (V. Colombo).

https://doi.org/10.1016/j.jormas.2025.102598
Received 13 March 2025; Accepted 5 October 2025
Available online 6 October 2025

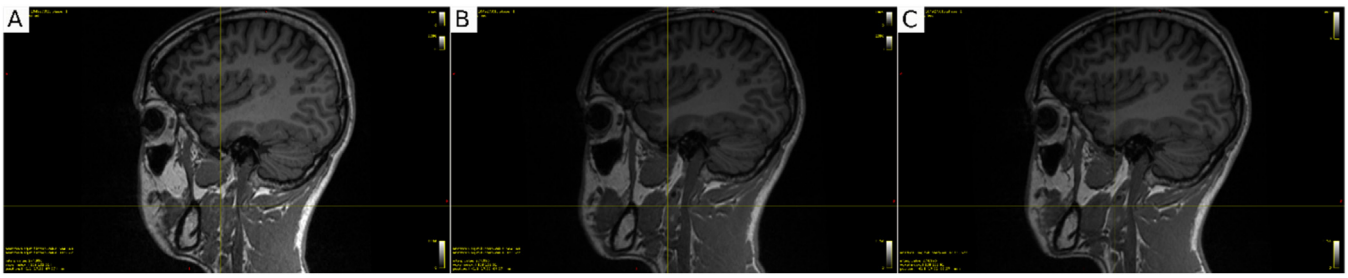


**Fig. 1.** Sagittal anatomical images of the subject in (A) $P_R$, (B) $P_{MID}$ and (C) $P_{MAX}$.

designed to provide a fixed, protruded position of the mandible while keeping the base of the tongue away from the posterior pharyngeal wall, thus preventing the collapse of the upper airway during sleep and reducing airflow resistance. MADs are generally better tolerated than CPAP systems on a long-term basis, and thus MADs may be used as an alternative to CPAP or even as a first-line treatment, especially in patients with mild or moderate OSA [12].

Although various long-term follow-up studies and literature reviews have reported skeletal side effects associated with the use of MAD, such as occlusal alterations, changes in overjet, overbite, tooth movements, and skeletal changes in the vertical dimension, the potential immediate and long-term effects of MAD use on the masticatory muscles (MM) remain undocumented in the literature [13,14].

Furthermore, the anatomical changes occurring in the airway space play a significant role in the efficacy of MAD therapy. Therefore, a clear understanding of the changes occurring with the increasing protrusion is crucial. The upper airway space has been studied in several clinical trials and at different positions of the head, but not observed intra-individually or at different degrees of protrusion in healthy individuals. The lack of knowledge about the effects of the protrusion on the geometrical and functional features of the MM, as well as in the upper airway space were the motivation for the present work.

The specific aim of this pilot study was to measure the fiber orientation of the masticatory muscles (superficial and deep head of masseter, anterior temporalis, medial and lateral pterygoid) and to assess the relevant morphometric features of the upper airway (volume, minimum cross-sectional area $CSA_{MIN}$) in three mandibular positions: habitual bite position ($P_R$ = 0 mm), middle protrusion ($P_{MID}$ = 3.5 mm), maximum protrusion ($P_{MAX}$ = 7 mm) in one healthy volunteer.

## 2. Materials and methods

### 2.1. Subject

One male subject, aged 24 years, with BMI 22.2, was recruited for this pilot study. The subject had no signs nor symptoms of temporomandibular disorders (TMD), assessed according to the standard diagnostic criteria for TMD (DC/TMD), no large metals in the mouth, jaw, or facial area (braces, piercings, or dental reconstructions), did not experience anxiety disorder, pathological condition of the dental apparatus or MRI contraindications. Written informed consent was obtained by the participant before the beginning of the study. This study followed the Declaration of Helsinki regarding medical protocols and ethics and was approved by the Ethics Committee of the Canton of Zurich (KEK-ZH—Nr. 2021−01277).

### 2.2. Study procedure

During the first appointment, a clinical examination was performed using a standardized procedure following the DC/TMD criteria to exclude the presence of signs or symptoms of TMD in the MM and/or the TMJ. Digital impressions of the maxillary and mandibular dental arches of the participant were then taken using a dental intraoral scanner (TRIOS, 3Shape, Denmark) and a bite registration was recorded at maximum intercuspal position. Afterwards, the digital scans were sent to an external company (ResMed Schweiz GmbH, Basel, Switzerland) for the fabrication of a personalized MAD (Narval CC™). Digital casts were then created and processed with CAD/CAM technology to design two full-arch splints, one for the maxillary and one for the mandibular dental arch. The splints were then produced via a laser-sintering 3D-printing procedure. The fabricated MAD was composed of highly resilient, durable, biocompatible polymer material free of allergenic substances such as parabens, Bisphenol A, metal, or latex. Mandibular protrusion was obtained through interchangeable rigid plastic rods of different lengths that were anchored on the buccal aspect of the MAD at the level of the premolar region allowing varying degrees of mandibular protrusion. For the study, three mandibular protrusions were selected: Reference position ($P_R$: 0 mm protrusion), mid-protrusion ($P_{MID}$: 3.5 mm) and maximum protrusion ($P_{MAX}$: 7 mm) (Fig. 1).

### 2.3. MRI

At a second appointment, a 3.0T scanner (MAGNETOM Prisma, Siemens Healthineers, Forchheim, Germany) was used to acquire the following sequences: 3D (isotropic) T1-weighted MPRAGE, and isotropic diffusion weighted single-shot echo planar imaging sequence. The parameters for the T1-weighted MPRAGE sequence were: Echo Time (TE) of 2.32 ms; Repetition Time (TR) of 2300 ms; Inversion Time (TI) of 900 ms; Field of View (FoV) read of 240 mm; FoV phase 100 %; Flip Angle of 8 degrees; and isotropic voxel size 0.9 × 0.9 × 0.9 mm. The parameters for the diffusion weighted imaging were: TE of 43.00 ms, TR of 6000 ms; FoV read 224 mm, FoV phase 120 %; Phase Encoding Direction Anterior >> Posterior; isotropic voxel size 2.8 × 2.8 × 2.8 mm; Monopolar diffusion scheme with 43 diffusion directions and b-value of 600 s/mm$^2$, including three non-diffusion weighted ($b$ = 0 s/mm$^2$) images. These scans were repeated for every mandibular position. Between imaging different mandibular positions, the participant left the scanner for the MAD to be adjusted to the new protruded position. The anatomical MRI scan was used to assess the status of the TMJ and exclude the presence of TMD. Additionally, cephalometric measurements were performed to characterize the subject's craniofacial morphology. The ANB angle was measured on the sagittal anatomical MRI scans. Angle classification (Class I/II/III) was recorded from the model obtained via digital impression. Mandibular plane−Sella−Nasion (SN-MP) angle was measured to classify the subject as hypodivergent, normodivergent, or hyperdivergent.

#### 2.3.1. DTI Fiber Tractography

For image post-processing and fiber tractography, FMRIB FSL v6.0.6 and MRtrix3 v3.0.3 were used [15,16]. Anatomical images were co-registered to the Montreal Neurological Institute (MNI) reference brain, MNI152 with a global transformation (rigid body transform with scaling) using FSL FLIRT, and the transforms and inverse transforms were recorded for subsequent shifting of tractography streamlines [17−20]. Eddy correction and denoising were applied to each DWI acquisition using FSL *eddy_correct* and *dwidenoise* functions. A response kernel was generated on a DWI scan with imaging area over the lower half of the head (i.e. excluding the brain) using the Tournier algorithm [21]. The

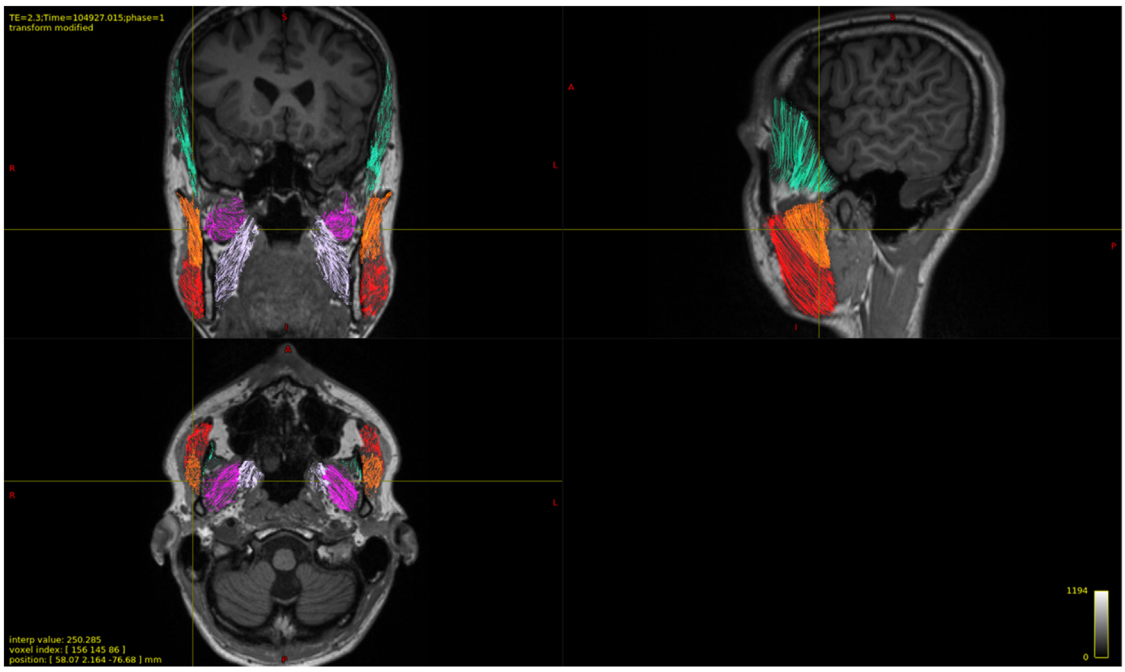


**Fig. 2.** MR Orthogonal View of anatomical images superimposed to muscles of mastication fiber tractography. Red: Superficial Head of Masseter muscle; Orange: Deep Head of Masseter muscle; Light green: Temporalis muscle; Magenta: Lateral Pterygoid muscle; Light Grey: Medial Pterygoid muscle.

kernel was then used to estimate the fiber orientation distribution (FOD) in each voxel by the constrained spherical deconvolution (CSD). The same kernel was used to generate the FOD images from DWI images for each jaw position (i.e. from the unregistered DWI images at $P_R$, $P_{MID}$, and $P_{MAX}$). Streamline tractography based on Spherical Deconvolution was performed on the FOD images using the MRTRIX3 *tckgen* command with the SD_STREAM algorithm. For each image, five million streamlines were generated throughout the entire image using a global seed mask (i.e. a cube shaped volumetric mask covering the entire head region, including all muscles). Streamlines were shifted to the reference brain position using the inverse transform of the associated anatomical registration. Inclusion and exclusion masks were manually drawn on co-

**Table 1**
Mean fiber orientation angles in three different positions and three planes on right and left side for masseter (deep, superficial head), medial pterygoid, lateral pterygoid, temporalis muscle.

| Muscle | Plane | Hand-side | $P_R$ (°) | $P_{MID}$ (°) | $P_{MAX}$ (°) |
|---|---|---|---|---|---|
| MASSETER DEEP | Sagittal | Left | 47.45 (11.74) | 70.24 (14.16) | 67.98 (11.41) |
| | | Right | 50.55 (10.34) | 70.56 (12.07) | 86.60 (12.93) |
| | Coronal | Left | 111.23 (5.52) | 112.09 (6.32) | 112.88 (2.44) |
| | | Right | 69.55 (2.30) | 70.38 (4.55) | 71.49 (4.55) |
| | Axial | Left | 114.37 (12.64) | 138.91 (24.25) | 135.61 (18.72) |
| | | Right | 64.12 (9.18) | 68.34 (80.69) | 140.31 (135.06) |
| MASSETER SUPERFICIAL | Sagittal | Left | 33.70 (8.60) | 42.49 (7.20) | 47.52 (9.25) |
| | | Right | 37.42 (5.16) | 47.09 (5.93) | 54.66 (6.20) |
| | Coronal | Left | 107.39 (17.35) | 105.35 (9.87) | 97.72 (10.89) |
| | | Right | 79.02 (17.92) | 77.58 (11.72) | 78.85 (7.83) |
| | Axial | Left | 99.94 (9.13) | 104.22 (10.61) | 93.59 (14.41) |
| | | Right | 82.37 (13.52) | 77.15 (13.72) | 77.36 (10.40) |
| MEDIAL PTERYGOID | Sagittal | Left | 41.99 (24.91) | 59.24 (10.61) | 56.93 (10.73) |
| | | Right | 40.56 (7.47) | 51.81 (7.27) | 63.27 (5.19) |
| | Coronal | Left | 52.44 (24.30) | 57.50 (8.54) | 51.24 (7.93) |
| | | Right | 132.35 (8.28) | 133.95 (7.61) | 125.93 (5.04) |
| | Axial | Left | 59.08 (26.52) | 49.52 (43.41) | 26.52 (7.60) |
| | | Right | 126.57 (7.29) | 141.05 (9.73) | 143.61 (6.24) |
| LATERAL PTERYGOID | Sagittal | Left | 138.31 (14.75) | 130.20 (26.72) | 138.18 (14.31) |
| | | Right | 138.14 (12.56) | 133.65 (20.54) | 140.35 (42.59) |
| | Coronal | Left | 132.69 (11.089 | 122.54 (26.88) | 142.50 (16.62) |
| | | Right | 41.04 (8.85) | 32.80 (12.59) | 62.13 (46.70) |
| | Axial | Left | 228.98 (12.83) | 210.66 (57.96) | 213.03 (15.35) |
| | | Right | 316.49 (16.97) | 336.15 (6.61) | 292.72 (59.13) |
| TEMPORALIS | Sagittal | Left | 98.85 (21.30) | 95.00 (20.90) | 97.81 (9.95) |
| | | Right | 93.70 (20.57) | 99.24 (20.95) | 96.72 (10.94) |
| | Coronal | Left | 102.39 (8.28) | 98.28 (9.35) | 95.76 (4.55) |
| | | Right | 81.64 (6.47) | 83.61 (10.92) | 81.77 (3.89) |
| | Axial | Left | 196.08 (50.57) | 183.01 (68.68) | 227.73 (51.98) |
| | | Right | 204.70 (123.78) | 229.82 (107.62) | 253.85 (106.18) |

Data are mean (SD); $P_R$ = Reference position; $P_{MID}$ = Mid-Protrusion; $P_{MAX}$ = Maximum protrusion; SD = Standard Deviation.

registered anatomical images in MRview. Separate masks were manually drawn based on the visible muscle anatomy as well as the insertion and origin points for the following muscles: deep and superficial heads of the masseter, temporalis, as well as medial and lateral pterygoid. Fibers were then selected for each MM from the shifted subset of 5 million fibers using the *tckedit* command (requesting up to 20,000 fibers per muscle) and using masks drawn as inclusion masks. In addition, airway volume in all three jaw positions was segmented, with the superior boundary defined as the start of the soft palate, and the inferior boundary defined as the superior margin of the epiglottis.

### 2.4. Quantitative analysis

Fiber tracts were imported into Matlab R2021a (The Mathworks Inc. Natick, MA, USA). Each tract consists of a vector of 3D position coordinates and used in the analysis were limited to having between 40 and

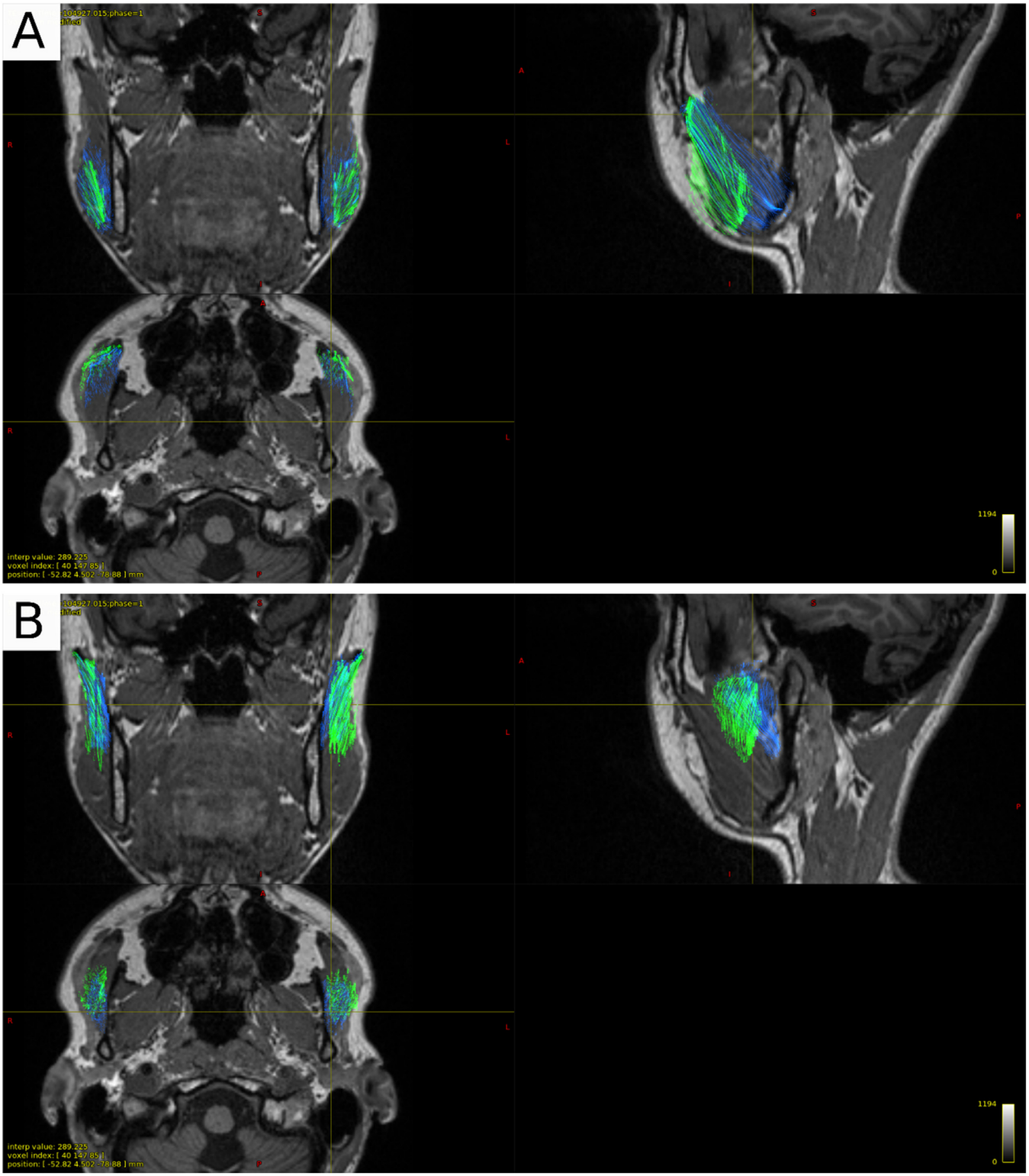


**Fig. 3.** MR Orthogonal View with fiber tractography of the superficial head of masseter (A), and deep head of masseter (B) for the position $P_R$ (blue) and $P_{MAX}$ (green).

500 sub-segments. For each muscle, fiber angles were calculated relative to a local coordinate system anchored to the inferior starting point of the fibers. (Supplementary: S1). A weighted distribution of the angles of all fibers, when projected onto the sagittal, coronal, and axial planes, was calculated to determine the main direction of each fiber in each plane. The distributions of all individual fiber angles were then examined to assess differences in angle for the superficial and deep heads of the masseter muscle, as well as the medial and lateral pterygoid muscles. For airway volume assessment, the pixels in the airway masks were summed and multiplied by the volume of each pixel. The minimum cross-sectional area ($CSA_{MIN}$) was calculated from the 3D airway volume as the smallest of the areas formed by the voxels in the axial plane. Airway volume and $CSA_{MIN}$ calculations were performed using custom scripts in Matlab R2021a.

## 3. Results

The anatomical scan showed no alteration of TMJ indicative of TMD. The subject exhibited an Angle Class I occlusion (overjet = 1 mm, overbite = 1 mm). Cephalometric analysis showed an angle ANB = 3.2°, consistent with a skeletal Class I pattern, and an angle SN-MP = 29.8°, indicating a normodivergent vertical skeletal phenotype.

Fiber tractography was obtained for all muscles of mastication in all positions. Following fiber tracking for each muscle specifically, and filtering based on length (number of sub-segments per fiber), a minimum of 350 fibers (maximum 1200, average 700 fibers) were used to calculate fiber angles in every position in each muscle (Fig. 2,Table 1).

The largest variations were observed for the superficial and deep heads of the masseter in the sagittal projection (Fig. 3, 4). The mean angle of the fibers of both muscle heads increased almost linearly with protrusion on both sides (about 20° for the deep head and 9° for the superficial head), becoming more craniocaudal, except for the right deep masseter head, whose values increased around 22° from $P_R$ to $P_{MID}$ but then dropped 2° from $P_{MID}$ to $P_{MAX}$. In the coronal and axial projections, less pronounced mean variations were observed. However, a higher standard deviation was noticed, particularly in the axial view for the deep muscle head, ranging from 9.18° to 135.06°.

The medial pterygoid showed a similar tendency as the masseter. In the sagittal projection, the fibers became more craniocaudally oriented (Fig. 5A). As with the deep masseter head, the angles on the left side increased from $P_R$ to $P_{MID}$ and then dropped at $P_{MAX}$. In the coronal projection, the fibers showed an asymmetrical behavior, becoming on average more craniocaudally oriented on the right side and more mediolateral on the left side, whereas for the axial projection, the angle distribution showed an increased anteroposterior direction from $P_{MID}$ to $P_{MAX}$.

The angles of the lateral pterygoid muscle revealed most pronounced changes in the coronal and axial planes (maximum variations of 29° in the coronal plane and 43° in the axial plane), with an initial drop from $P_R$ to $P_{MID}$ and an increase from $P_{MID}$ to $P_{MAX}$ with high asymmetrical increase/decrease in the craniocaudal direction depending on the side, and large standard deviation. In general, the angles showed an initial change toward a medio-lateral position of the fibers and then a more anteroposterior for the right side and vice versa for the left side (Fig. 5B).

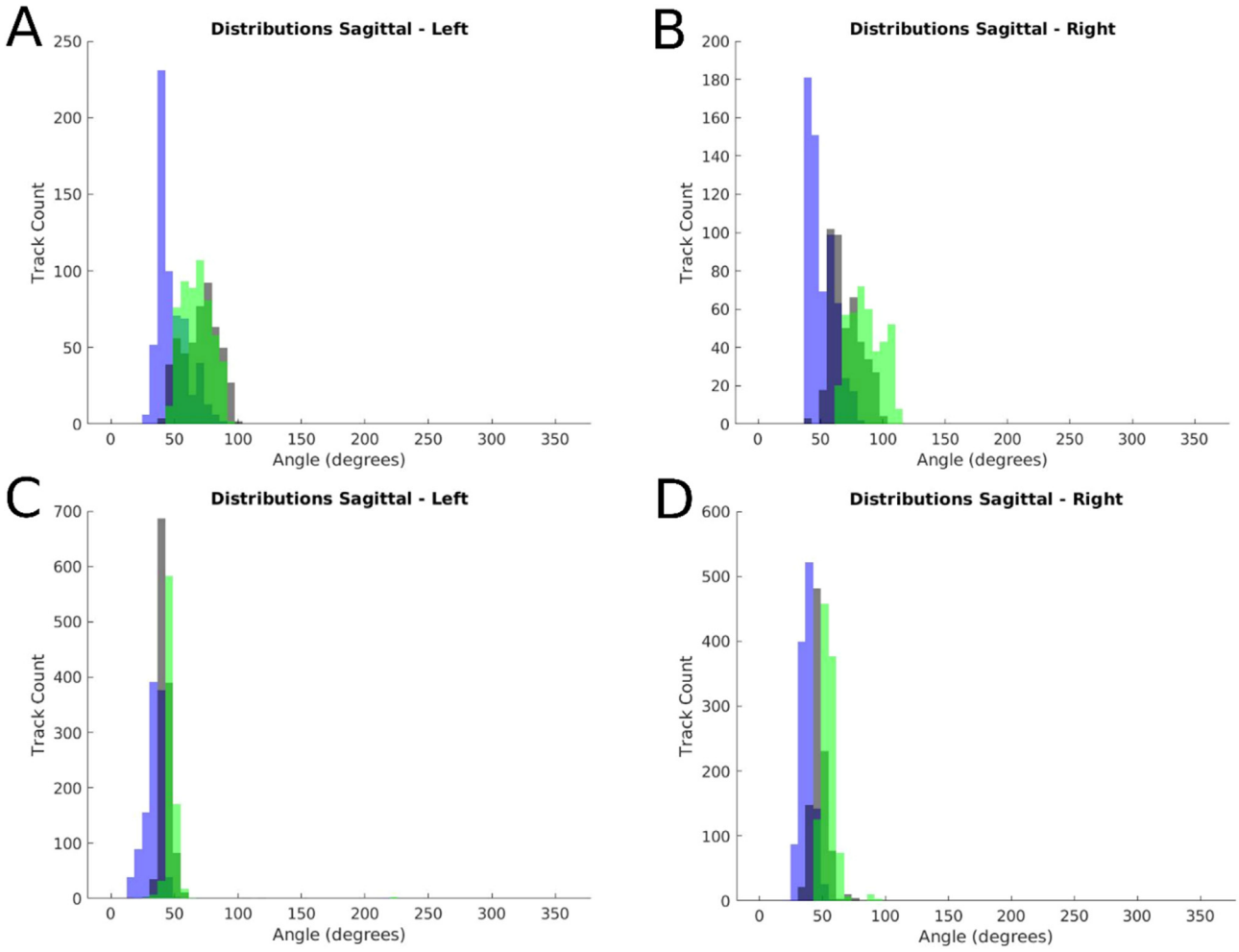


**Fig. 4.** Distribution of the fibers' angle in the sagittal plane for left side (LHS) (left column) and right side (RHS) (right column) for the deep (A, B) and superficial (C, D) head of masseter muscle in the three analyzed positions: $P_R$ (blue), $P_{MID}$ (gray) and $P_{MAX}$ (green).

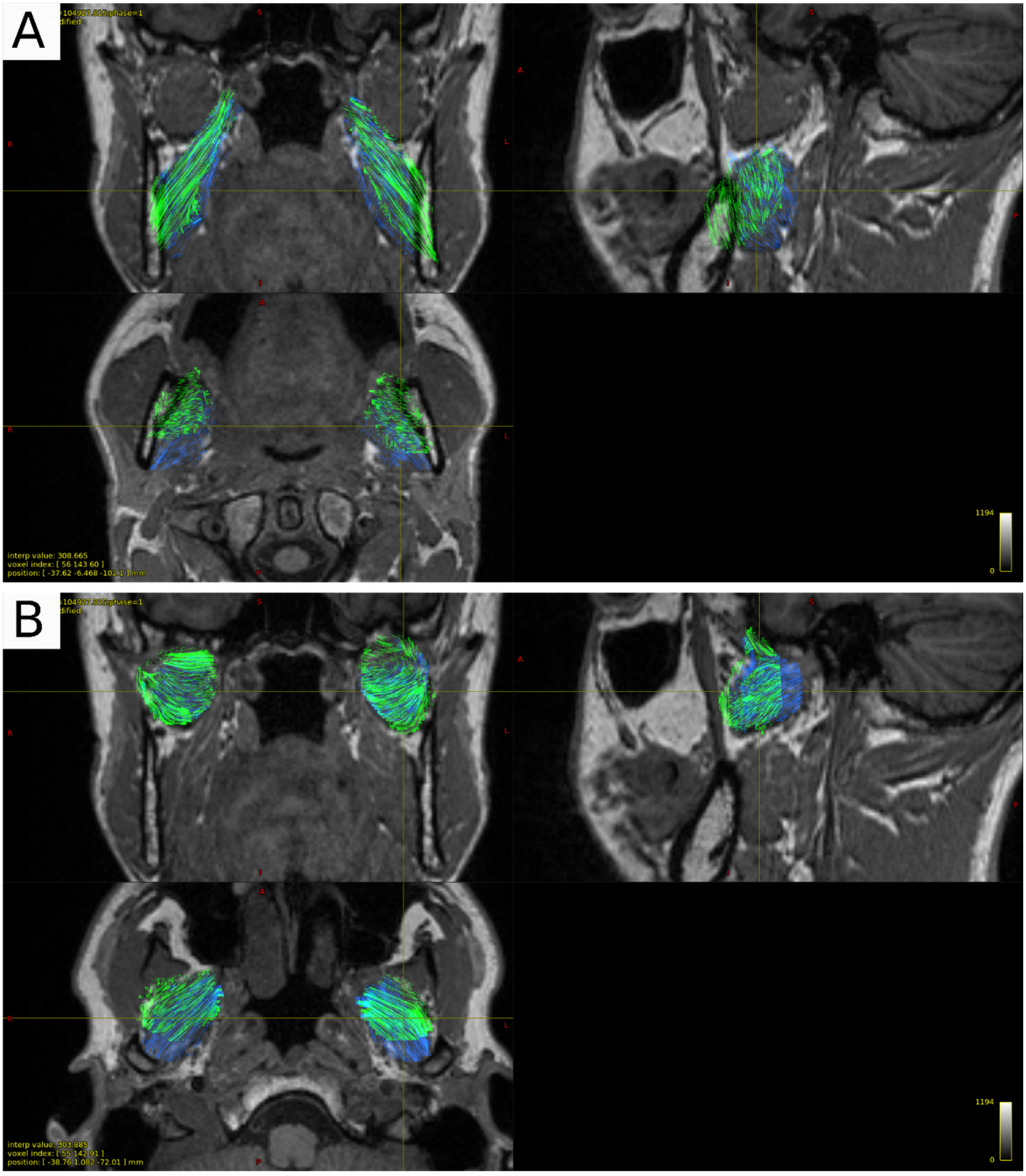


**Fig. 5.** MR Ortho View with fiber tractography of the medial pterygoid (A), and lateral pterygoid (B) for the position $P_R$ (blue) and $P_{MAX}$ (green).

The average angle of the fibers of the temporalis increased mainly in the axial projection on both sides. The primary change in the fiber orientation was at the insertion points (Fig. 6).

The total airway volume was 11.74 $cm^3$, 15.70 $cm^3$, and 19.09 $cm^3$ at $P_R$, $P_{MID}$, and $P_{MAX}$, respectively and increased almost linearly with protrusion (around 0.4 $cm^3$ per protrusion step). The change can be seen in all planes in the anatomical for $P_R$ and $P_{MAX}$ (Fig. 7). The $CSA_{MIN}$ was 0.79 $cm^2$, 2.37 $cm^2$, and 2.48 $cm^2$ at $P_R$, $P_{MID}$, and $P_{MAX}$, respectively, increasing 1.6 $cm^2$ from $P_R$ to $P_{MID}$, but then only 0.1 $cm^2$ from $P_{MID}$ to $P_{MAX}$.

## 4. Discussion

To the best of our knowledge, this is the first quantitative description of the effects of different MAD-induced mandibular protrusions on the orientation of the MM and the airway volume in one healthy subject,

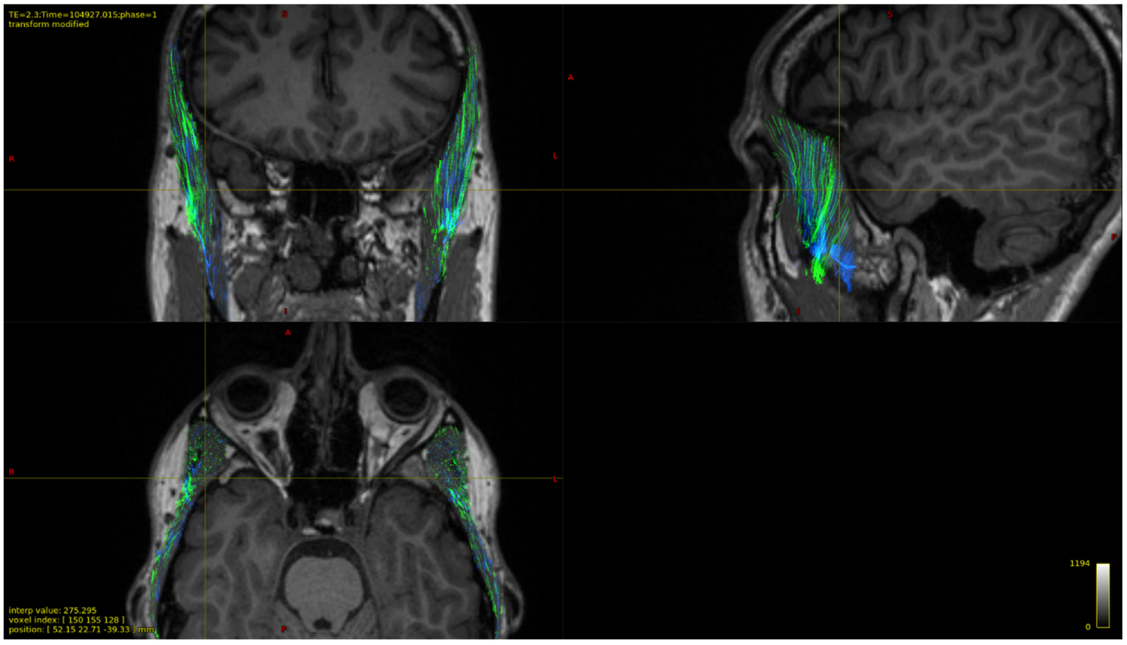


**Fig. 6.** MR Ortho View of the attachment points of the temporalis muscle for the mandible in the rest position $P_R$, (blue) and in the most advanced position $P_{MAX}$, (green).

using DTI as a non-invasive method for measuring the orientation of the MM fibers as described by Sugano et al. [22]. This pilot study was conducted with the main aim of defining the appropriate methods and the parameters to evaluate and analyze the influence of the mandibular positions on the orientation and angle of the fibers of the MM and the change in the volume of the airway space.

The main findings of our analysis showed that the MAD controlled protrusion caused variations of the angles of the fibers of all MM (Figs. 2,3,5 and 6), with a value depending on the observed muscle and the mandibular position. Generally, the changes were more marked between $P_R$ and $P_{MAX}$. In the sagittal projection, the orientation of the muscle fibers of the superficial and deep masseter, and the medial pterygoid became more vertical with increasing protrusion, with a linear increase for the muscle of the left side (Fig. 2,5). Unexpectedly, on the right side, the angles were maximal at $P_{MID}$ and then dropped to a lower value at $P_{MAX}$. This drop might be attributed to an asymmetrical anterior translation of the condylar heads in the TMJs, with a more restricted condylar movement on the right side. The same pattern was followed by the medial pterygoid. Other muscles showed less pronounced changes of the fiber angles in the sagittal direction. In the sagittal projection, the lateral pterygoid muscle fiber orientations were slightly influenced by the level of protrusion, whereas maximum changes were observed in the coronal and axial planes. During protrusion, the orientation of the fibers of the lateral pterygoid tend to become more mediolaterally oriented, because the anterior movement causes the insertion of the muscle fibers to shift more laterally relative to their origin [23]. In this case, an asymmetrical change was observed for the direction of the medial and lateral pterygoid fibers. Also in this case, changes can be due to an asymmetrical forward translation of the condyles.

The maximum protrusion of the subject was 7 mm, that represents as slightly limited protrusion, if compared to the physiological ranges of mandibular protrusion generally observed in the clinical setting, might have impacted the results of both angles and upper airway volume [24].

A previous DTI study analyzing fiber angle changes in the masseter muscle at rest and after mandibular opening reported an increase in fiber orientation in the frontal plane and a slight, though not statistically significant, increase in the sagittal plane [25]. The authors suggested that these regional differences in angle changes may indicate functional compartmentalization within the muscle. In our subject, we also observed regional variation in masseter fiber changes during protrusion, particularly in the sagittal plane, which aligns with the anteroposterior nature of mandibular protrusion. These findings support the notion that masseter muscle architecture may adapt differentially, based on functional demands and jaw movement direction.

The association between increased oropharyngeal volume after MAD application and reduction of OSA symptoms has already been described in different studies [26−29]. Therefore, MAD have been considered a valid alternative treatment to CPAP for patient with mild or moderate OSA [12]. Also in our case, the use of MAD was associated with an increase of the upper airway dimension. The upper airway cross-sectional area is known to be narrowed in patients suffering from OSA [30−32]. Furthermore, its increase is considered a key predictor for a positive treatment outcome in patients experiencing OSA [12,33,34]. For this reason, besides the total airway volume, the minimum cross-sectional area of the upper airway was chosen as a key metric in our study.

In our subject, both airway volume and $CSA_{MIN}$ increased after the application of the MAD. However, while $V_{TOT}$ increased almost linearly with increasing protrusion, the $CSA_{MIN}$ was affected by a greater variation in the first 50 % of the maximum protrusion $P_{MID}$ and changed only slightly from $P_{MID}$ to $P_{MAX}$. A possible explanation of the non-linear increase of the $CSA_{MIN}$ might be attributed to motion or respiratory artifacts during the MRI scan. Although a study by Yucel et al. using dynamic CT scans has shown that the value of $CSA_{MIN}$ in OSA patients can be influenced by the respiration phases, the changes in the $CSA_{MIN}$ found by Yucel et al. at the level of the uvula between tidal breathing and forced expiration/inspiration did not exceed 0.3 $cm^2$, which is less than variation induced by protrusion in our case between $P_R$ and $P_{MID}$, (1.58 $cm^2$) and therefore not sufficient to explain the increase between baseline and the first level of protrusion. However, it may have negatively influenced the changes between $P_{MID}$ and $P_{MAX}$ (0.11 $cm^2$) [29].

Different head positions have also been shown to affect the airway space during measurements. However, the changes observed in the three different mandibular protrusions are unlikely to be attributed to changes in the head posture, as the position assumed by the subject was neutral and maintained for all three scans [35,36].

A study on protrusion optimization was conducted by Dort et al. in 2006, to identify the effective protrusion for MAD therapy during a routine Polysomnographic examination. Their findings showed that

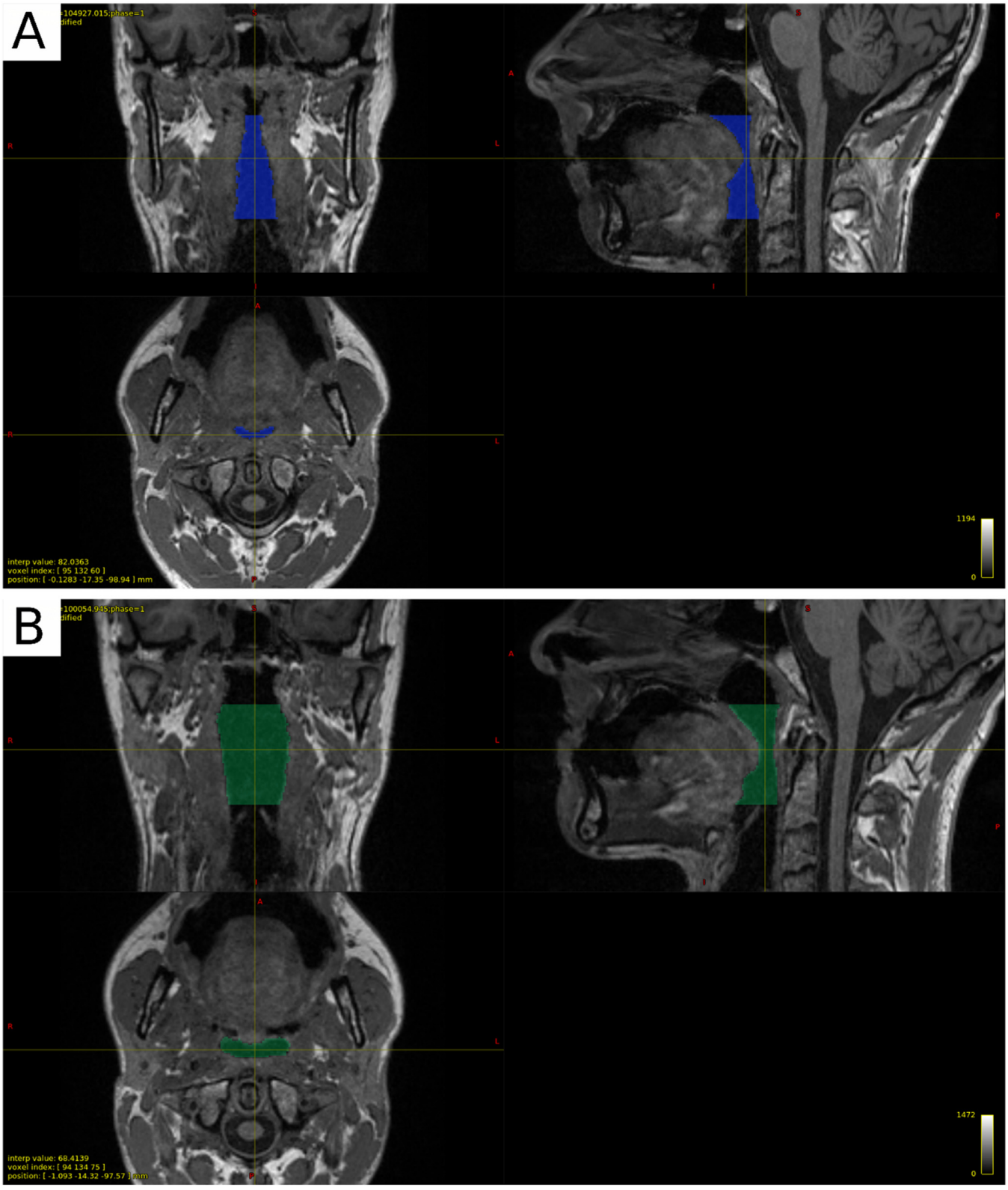


**Fig. 7.** MR Orthogonal view of the airway volume for the rest position (A) $P_R$ (blue) and for (B) $P_{MAX}$ (green).

therapeutic success was achieved with an average protrusion of 6.3 mm on a maximum clinically measured average protrusion of 8.6 mm, representing 73 % of the average maximum protrusion in their sample [37]. However, we couldn't observe an increase of $CSA_{MIN}$ for more than 50 % of the maximum protrusion. Therefore, the causes of a non-linear increase might be due to the specific anatomy of the subject and raises the question of optimising the level of protrusion selected for the use of MAD in clinical applications.

In our study, the airway dimensions were assessed using MRI, which is a safe, non-ionising, reliable tool for visualising soft tissues. In contrast with cone-beam CT, which is usually employed for craniofacial measurements, MRI has the advantage of being performed with the subject in a

supine position, mimicking the sleeping condition. Furthermore, previous studies which evaluated craniofacial parameters with CBCT in comparison to MRI obtained comparable results, indicating that this method can be considered representative for the evaluation of the upper airway structures [38,39].

Our results at baseline are also comparable with those of a previous study who measured the upper airway volume in healthy controls, finding an average pharyngeal volume of 17,415.42 $mm^3$ [40]. In Ciscar et al., the $CSA_{MIN}$ measured with an MRI technique was on average 103.2 ± 10 $mm^2$ for healthy controls, which is also in line with our results [41].

Our finding of an increased total upper-airway volume and $CSA_{MIN}$ with mandibular advancement is also consistent with previous three-dimensional imaging studies evaluating MAD therapy in OSA patients. These studies have reported clinically relevant increases in both airway volume and $CSA_{MIN}$ after protrusion [27,28], supporting the potential functional relevance of our results in the context of OSA treatment. In this context, our pilot study provides support for the hypothesis that the therapeutic effect of MADs at least partially relies on the increase of the upper airway dimension. Still, a recent study by Shi et al. comparing the upper airway dimensions between MAD responders and non-responders with mild or moderate OSA reported no significant differences between the two groups, indicating that a change of the upper airway dimensions does not necessarily result in a change of the apnea-hypopnea index [42].

The main limitation of this study is that the protruded position of the mandible was passively provided by the MAD, and the reference for the protrusion may have been based on a position different from the effective anatomical position of the condyle during sleep.

The subject in this study presented with a normodivergent facial type and a sagittal relationship matching Class I. This relatively balanced skeletal and occlusal morphology suggests that the observed muscle and airway changes were unlikely to be confounded by extreme skeletal discrepancies. Since the present findings are based on a subject with average morphology, caution should be taken in generalizing the results to populations with more pronounced skeletal or occlusal variations. Additionally, as the analysis was performed in a single imaging session, the potential long-term effects of MAD use on muscle morphology were not addressed. Therefore, it remains unclear whether the effect of MAD on the MM will persist over longer periods of MAD use.

Future research with larger and more phenotypically diverse samples is needed to evaluate how differences in sagittal and vertical skeletal relationships, and the skeletal versus dental origins of overjet and overbite, might affect outcomes. Such work, in conjunction with longitudinal observations, would provide a clearer understanding of the variability in responses across different craniofacial types over time. In addition, studies integrating structural diffusion tensor imaging (DTI) data with functional assessments, such as electromyography (EMG) recordings or bite-force measurements could enable direct correlation between observed changes in masticatory muscle fiber orientation and actual muscle activity or force generation.

In conclusion, this pilot study using DTI provided initial mechanistic insight into the effect of MAD on the MM architecture and the upper airway dimensions, both of which are considered key factors in the OSA treatment. These preliminary findings suggest the potential utility of personalized MAD therapy in OSA management. Current results, based on a single subject, should be confirmed in a larger phenotype-stratified cohort and account for functional and long-term outcomes.

## Funding

This work was supported by the standard financial plan of the University of Zurich and by ResMed Schweiz GmbH, Switzerland.

## Declaration of competing interest

The authors declare that they have no known competing financial interests or personal relationships that could have appeared to influence the work reported in this paper.

## CRediT authorship contribution statement

**Daria Madanchi:** Writing – review & editing, Writing – original draft, Visualization, Investigation, Data curation. **Catherine M. Paverd:** Writing – review & editing, Visualization, Validation, Software, Methodology, Formal analysis, Data curation. **Constantin von Deuster:** Writing – review & editing, Validation, Resources, Methodology. **Stefan Sommer:** Writing – review & editing, Validation, Resources, Methodology. **Marga B. Rominger:** Writing – review & editing, Conceptualization. **Dominik A. Ettlin:** Writing – review & editing, Resources, Methodology, Conceptualization. **Luigi M. Gallo:** Writing – review & editing, Supervision, Conceptualization. **Vera Colombo:** Writing – review & editing, Supervision, Resources, Project administration, Methodology, Investigation, Conceptualization.

## Supplementary materials

Supplementary material associated with this article can be found, in the online version, at doi:10.1016/j.jormas.2025.102598.

## References

[1] Mehta A, Qian J, Petocz P, Darendeliler MA, Cistulli PA. A randomized, controlled study of a mandibular advancement splint for obstructive sleep apnea. Am. J. Respir. Crit. Care Med 2001;163(6):1457–61. doi: 10.1164/ajrccm.163.6.2004213.
[2] Tsara V, Amfilochiou A, Papagrigorakis MJ, Georgopoulos D, Liolios E. Guidelines for diagnosis and treatment of sleep-related breathing disorders in adults and children. Definition and classification of sleep related breathing disorders in adults: different types and indications for sleep studies (Part 1). Hippokratia 2009;13(3):187–91 https://pubmed.ncbi.nlm.nih.gov/19918312/.
[3] Peppard PE, Young T, Palta M, Skatrud J. Prospective study of the association between sleep-disordered breathing and hypertension. N Engl J Med 2000;342 (19):1378–84. doi: 10.1056/NEJM200005113421901.
[4] Gottlieb DJ, Yenokyan G, Newman AB, et al. Prospective study of obstructive sleep apnea and incident coronary heart disease and heart failure: the sleep heart health study. Circulation 2010;122(4):352–60. doi: 10.1161/CIRCULATIONAHA.109.901801.
[5] Yaggi HK, Concato J, Kernan WN, Lichtman JH, Brass LM, Mohsenin V. Obstructive sleep apnea as a risk factor for stroke and death. N Engl J Med 2005;353(19):2034–41. doi: 10.1056/NEJMoa043104.
[6] Basyuni S, Barabas M, Quinnell T. An update on mandibular advancement devices for the treatment of obstructive sleep apnoea hypopnoea syndrome. J Thorac Dis 2018;10(Suppl 1):S48–56. doi: 10.21037/jtd.2017.12.18.
[7] Patil SP, Ayappa IA, Caples SM, Kimoff RJ, Patel SR, Harrod CG. Treatment of Adult Obstructive Sleep Apnea with Positive Airway Pressure: an American Academy of Sleep Medicine Clinical Practice Guideline. J Clin Sleep Med 2019;15(2):335–43. doi: 10.5664/jcsm.7640.
[8] Fujita Y, Yamauchi M, Muro S. Assessment and management of continuous positive airway pressure therapy in patient with obstructive sleep apnea. Respir Investig 2024;62(4):645–50. doi: 10.1016/j.resinv.2024.05.004.
[9] Bikov A, Bentley A, Csoma B, Smith N, Morris B, Bokhari S. Long-Term Adherence to Continuous Positive Airway Pressure in Patients with Obstructive Sleep Apnoea Set Up in a Complete Remote Pathway: a Single-Centre Service Evaluation Project. J Clin Med 2024;13(10). doi: 10.3390/jcm13102891.
[10] Rotenberg BW, Murariu D, Pang KP. Trends in CPAP adherence over twenty years of data collection: a flattened curve. J Otolaryngol Head Neck Surg 2016;45(1):43. doi: 10.1186/s40463-016-0156-0.
[11] Weaver TE, Maislin G, Dinges DF, et al. Relationship between hours of CPAP use and achieving normal levels of sleepiness and daily functioning. Sleep 2007;30(6):711–9. doi: 10.1093/sleep/30.6.711.
[12] Ramar K, Dort LC, Katz SG, et al. Clinical Practice Guideline for the Treatment of Obstructive Sleep Apnea and Snoring with Oral Appliance Therapy: an Update for 2015. J Clin Sleep Med 2015;11(7):773–827. doi: 10.5664/jcsm.4858.
[13] Martins Olivia de Freitas Mendes, Chaves Junior CM, Rossi RRP, Cunali PA, Dal-Fabbro C, Bittencourt L. Side effects of mandibular advancement splints for the treatment of snoring and obstructive sleep apnea: a systematic review. Dent. Press J Orthod 2018;23(4):45–54. doi: 10.1590/2177-6709.23.4.045-054.oar.
[14] Martínez-Gomis J, Willaert E, Nogues L, Pascual M, Somoza M, Monasterio C. Five years of sleep apnea treatment with a mandibular advancement device. Side effects and technical complications. Angle Orthod 2010;80(1):30–6. doi: 10.2319/030309-122.1.
[15] Smith SM, Jenkinson M, Woolrich MW, et al. Advances in functional and structural MR image analysis and implementation as FSL. NeuroImage 2004;23(Suppl 1): S208–19. doi: 10.1016/j.neuroimage.2004.07.051.
[16] Tournier J-D, Smith R, Raffelt D, et al. MRtrix3: a fast, flexible and open software framework for medical image processing and visualisation. NeuroImage 2019;202:116137. doi: 10.1016/j.neuroimage.2019.116137.

[17] Fonov VS, Evans AC, McKinstry RC, Almli CR, Collins DL. Unbiased nonlinear average age-appropriate brain templates from birth to adulthood. NeuroImage 2009;47:S102. doi: 10.1016/S1053-8119(09)70884-5.
[18] Fonov V, Evans AC, Botteron K, Almli CR, McKinstry RC, Collins DL. Unbiased average age-appropriate atlases for pediatric studies. NeuroImage 2011;54(1):313–27. doi: 10.1016/j.neuroimage.2010.07.033.
[19] Jenkinson M, Smith S. A global optimisation method for robust affine registration of brain images. Med Image Anal 2001;5(2):143–56. doi: 10.1016/s1361-8415(01)00036-6.
[20] Jenkinson M, Bannister P, Brady M, Smith S. Improved optimization for the robust and accurate linear registration and motion correction of brain images. NeuroImage 2002;17(2):825–41. doi: 10.1016/s1053-8119(02)91132-8.
[21] Tournier J-D, Calamante F, Connelly A. Determination of the appropriate b value and number of gradient directions for high-angular-resolution diffusion-weighted imaging. NMR Biomed 2013;26(12):1775–86. doi: 10.1002/nbm.3017.
[22] Sugano T, Yoda N, Ogawa T, et al. Application of Diffusion Tensor Imaging Fiber Tractography for Human Masseter Muscle. Tohoku J Exp Med 2022;256(2):151–60. doi: 10.1620/tjem.256.151.
[23] Usui A, Akita K, Yamaguchi K. An anatomic study of the divisions of the lateral pterygoid muscle based on the findings of the origins and insertions. Surg Radiol Anat 2008;30(4):327–33. doi: 10.1007/s00276-008-0329-2.
[24] Mayoral P, Lagravère MO, Míguez-Contreras M, Garcia M. Antero-posterior mandibular position at different vertical levels for mandibular advancing device design. BMC Oral Health 2019;19(1):85. doi: 10.1186/s12903-019-0783-8.
[25] Sugano T, Ogawa T, Yoda N, et al. Morphological comparison of masseter muscle fibres in the mandibular rest and open positions using diffusion tensor imaging. J Oral Rehabil 2022;49(6):608–15. doi: 10.1111/joor.13319.
[26] Verma A, Jain S. Efficacy of Mandibular Advancement Device in the Treatment of Obstructive Sleep Apnoea by Evaluating Upper Airway Space Volume Using CBCT. J Coll Physicians Surg Pak 2023;33(10):1194–7. doi: 10.29271/jcpsp.2023.10.1194.
[27] Venza N, Malara A, Liguori C, Cozza P, Laganà G. Upper Airway Characteristics and Morphological Changes by Different MADs in OSA Adult Subjects Assessed by CBCT 3D Imaging. J Clin Med 2023;12(16). doi: 10.3390/jcm12165315.
[28] Shete CS, Bhad WA. Three-dimensional upper airway changes with mandibular advancement device in patients with obstructive sleep apnea. Am J Orthod Dentofac. Orthop 2017;151(5):941–8. doi: 10.1016/j.ajodo.2016.09.025.
[29] Marco-Pitarch R, García-Selva M, Plaza-Espín A, et al. Dimensional analysis of the upper airway in obstructive sleep apnoea syndrome patients treated with mandibular advancement device: a bi- and three-dimensional evaluation. J Oral Rehabil 2021;48(8):927–36. doi: 10.1111/joor.13176.
[30] Yucel A, Unlu M, Haktanir A, Acar M, Fidan F. Evaluation of the upper airway cross-sectional area changes in different degrees of severity of obstructive sleep apnea syndrome: cephalometric and dynamic CT study. AJNR Am J Neuroradiol 2005;26(10):2624–9.
[31] Pépin JL, Veale D, Ferretti GR, Mayer P, Lévy PA. Obstructive sleep apnea syndrome: hooked appearance of the soft palate in awake patients—cephalometric and CT findings. Radiology 1999;210(1):163–70. doi: 10.1148/radiology.210.1.r99ja10163.
[32] Jäger L, Günther E, Gauger J, Reiser M. Fluoroscopic MR of the pharynx in patients with obstructive sleep apnea. AJNR Am J Neuroradiol 1998;19(7):1205–14.
[33] Hartfield PJ, Janczy J, Sharma A, et al. Anatomical determinants of upper airway collapsibility in obstructive sleep apnea: a systematic review and meta-analysis. Sleep Med Rev 2023;68:101741. doi: 10.1016/j.smrv.2022.101741.
[34] Zreaqat M, Hassan R, Alforaidi S, Kassim NK. Effects of rapid maxillary expansion on upper airway parameters in OSA children with maxillary restriction: a CBCT study. Pediatr Pulmonol 2024;59(10):2490–8. doi: 10.1002/ppul.27050.
[35] Tsuiki S, Almeida FR, Lowe AA, Su J, Fleetham JA. The interaction between changes in upright mandibular position and supine airway size in patients with obstructive sleep apnea. Am J Orthod Dentofac. Orthop 2005;128(4):504–12. doi: 10.1016/j.ajodo.2004.03.040.
[36] Gurani SF, Cattaneo PM, Rafaelsen SR, Pedersen MR, Thorn JJ, Pinholt EM. The effect of altered head and tongue posture on upper airway volume based on a validated upper airway analysis-An MRI pilot study. Orthod Craniofac Res 2020;23(1):102–9. doi: 10.1111/ocr.12348.
[37] Dort LC, Hadjuk E, Remmers JE. Mandibular advancement and obstructive sleep apnoea: a method for determining effective mandibular protrusion. Eur Respir J 2006;27(5):1003–9. doi: 10.1183/09031936.06.00077804.
[38] Barrera JE, Pau CY, Forest V-I, Holbrook AB, Popelka GR. Anatomic measures of upper airway structures in obstructive sleep apnea. World J Otorhinolaryngol Head Neck Surg 2017;3(2):85–91. doi: 10.1016/j.wjorl.2017.05.002.
[39] Juerchott A, Freudlsperger C, Weber D, et al. In vivo comparison of MRI- and CBCT-based 3D cephalometric analysis: beginning of a non-ionizing diagnostic era in craniomaxillofacial imaging? Eur Radiol 2020;30(3):1488–97. doi: 10.1007/s00330-019-06540-x.
[40] Anandan R, Lakshmi KC, Ganesan A, AniyanK Y. Assessment of pharyngeal airway space with MRI In oral submucous fibrosis: a cross-sectional observational study. J Oral Biol Craniofac Res 2024;14(6):669–75. doi: 10.1016/j.jobcr.2024.09.003.
[41] Ciscar MA, Juan G, Martínez V, et al. Magnetic resonance imaging of the pharynx in OSA patients and healthy subjects. Eur Respir J 2001;17(1):79–86. doi: 10.1183/09031936.01.17100790.
[42] Shi X, Lobbezoo F, Chen H, et al. Effects of mandibular advancement devices on upper airway dimensions in obstructive sleep apnea: responders versus non-responders. Clin Oral Investig 2023;27(9):5649–60. doi: 10.1007/s00784-023-05186-w.